Journal of Power Sources 195 (2010) 7323–7331

Contents lists available at ScienceDirect

Journal of Power Sources

journal homepage: www.elsevier.com/locate/jpowsour

Open circuit voltage durability study and model of catalyst coated membranes at different humidification levels

Sumit Kundu[a,*], Michael W. Fowler[a], Leonardo C. Simon[a], Rami Abouatallah[b], Natasha Beydokhti[b]

[a] Department of Chemical Engineering, University of Waterloo, 200 University Avenue West, Waterloo, Ontario, Canada N2L 3G1
[b] Hydrogenics Corporation, 5985 McLaughlin Road, Mississauga, Ontario, Canada L5R 1B8

ARTICLE INFO

Article history:
Received 9 March 2010
Received in revised form 12 May 2010
Accepted 13 May 2010
Available online 20 May 2010

Keywords:
Chemical degradation
Degradation model
Fluoride release
Fuel cell durability

ABSTRACT

Fuel cell material durability is an area of extensive research today. Chemical degradation of the ionomer membrane is one important degradation mechanism leading to overall failure of fuel cells. This study examined the effects of relative humidity on the chemical degradation of the membrane during open circuit voltage testing. Five Gore™ PRIMEA® series 5510 catalyst coated membranes were degraded at 100%, 75%, 50%, and 20% RH. Open circuit potential and cumulative fluoride release were monitored over time. Additionally scanning electron microscopy images were taken at end of the test. The results showed that with decreasing RH fluoride release rate increased as did performance degradation. This was attributed to an increase in gas crossover with a decrease in RH. Further, it is also shown that interruptions in testing may heavily influence cumulative fluoride release measurements where frequent stoppages in testing will cause fluoride release to be underestimated. SEM analysis shows that degradation occurred in the ionomer layer close to the cathode catalyst. A chemical degradation model of the ionomer membrane was used to model the results. The model was able to predict fluoride release trends, including the effects of interruptions, showing that changes in gas crossover with RH could explain the experimental results.

1. Introduction

In order to be suitable for commercialization polymer electrolyte membrane (PEM) fuel cells must be able to operate for 5000 h in automotive applications [1] and over 40,000 h in stationary applications [2]. For this reason, fuel cell material reliability and durability are a few of several issues facing fuel cell commercial viability and as such have been the topic of increasing research. Durability issues in fuel cells range from catalyst degradation from start-up/shutdown transients to chemical attack of the polymer chains and have been extensively reviewed by several authors [3–5].

One of the most common forms of fuel cell material degradation is chemical degradation of the PFSA ionomer membrane consisting of radical attack of reactive endgroups on the polymer backbone as follows [6]:

Step 1:	$R–CF_2COOH + OH^{\bullet} \rightarrow R–CF_2^{\bullet} + CO_2 + H_2O$
Step 2:	$R–CF_2^{\bullet} + OH^{\bullet} \rightarrow R–CF_2OH \rightarrow R–COF + HF$
Step 3:	$R–COF + H_2O \rightarrow R–COOH + HF$

Studies have also indicated that the sulphonic acid sites in Nafion® are also vulnerable to radical attack [7]. Common observations from chemical degradation include fluoride release as suggested by the above mechanism, membrane thinning, as well as an increase in gas crossover from thinning or pinhole formation.

The radicals themselves are considered to be generated by a Fenton's type reaction whereby metal ions present in the membrane and peroxide generated by the combination of crossover gasses combine to form radicals. It is not yet clear where the peroxide is generated. The anode has a potential favourable to peroxide production from oxygen crossover [8]. It has also been proposed that crossover oxygen and/or hydrogen may combine directly to create degrading chemical species [9]. The production of peroxide and radicals at platinum bands within the membrane from hydrogen and oxygen permeating through the membrane has also been proposed [8,10–12]. Recently Hasegawa et al. [13] performed experiments on membranes with and without a platinum band and concluded that radicals were potentially generated at both electrode and band locations. Irrespective of the location of peroxide generation there is clear evidence that gas crossover is one of the main drivers of the degradation. Gas crossover in fuel cell membranes results from a combination of the gas partial pressures, gas permeability, and membrane thickness and has been shown to follow Fick's law as shown in (1) [14–16].

$$N_i = P_{M,i}\frac{\Delta p_i}{\delta_m} \quad (1)$$

Experimental studies on the effect of permeability, thickness, and relative humidity have been shown to impact chemical degra-

* Corresponding author.
E-mail address: s2kundu@uwaterloo.ca (S. Kundu).

0378-7753/$ – see front matter © 2010 Elsevier B.V. All rights reserved.
doi:10.1016/j.jpowsour.2010.05.027

Nomenclature

C_{F^-}	fluoride ion concentration, mol cm^{-3}
D_i	diffusion coefficient of species i, cm^2 s^{-1}
D_{GDL}	fluoride diffusion coefficient through the GDL, cm^2 s^{-1}
D_I	fluoride diffusion coefficient through the ionomer, cm^2 s^{-1}
E_{OCV}	open circuit voltage, V
E_{Nernst}	Nernst potential, V
EAS	electrochemically active surface area per unit geometric surface area, m^2 m^{-2}
EAS^0	initial electrochemically active surface area per unit geometric surface area, m^2 m^{-2}
F	Faraday's constant, C mol^{-1}
f_I	cathode ionomer fraction
F_C	cumulative fluoride release per unit geometric surface area, mol cm^{-2}
i_{H_2}	crossover current per unit geometric surface area, A cm^{-2}
$i^0_{H_2}$	initial crossover current per unit geometric surface area, A cm^{-2}
i_o	exchange current density per active surface area, A cm^{-2}
K_1	proportionality constant, cm^2 mol^{-1}
K_2	proportionality constant, mol cm^{-2}
K_3	proportionality constant
k_{H_2}	hydrogen permeability constant, mol cm cm^{-2} mm Hg^{-1} s^{-1}
k'_{H_2}	hydrogen permeability constant A, cm cm^{-2} mm Hg^{-1}
N_{F^-}	fluoride ion flux, mol cm^{-2} s^{-1}
N_{H_2}	hydrogen flux, mol cm^{-2} s^{-1}
N_{OH}	OH radical flux, mol cm^{-2} s^{-1}
n_{F^-}	mols of fluoride ion per geometric surface area, mol cm^{-2}
Δp_{H_2}	hydrogen pressure differential, mm Hg
R	ideal gas constant, J mol^{-1} K^{-1}
T	temperature, K
x	distance from anode channel, cm
δ	total ionomer membrane thickness, cm
δ_{GDL}	GDL thickness, cm
δ_{IA}	anode ionomer thickness, cm
δ^0_{IC}	initial cathode ionomer thickness, cm
γ	crossover current modifier
$\eta_{crossover}$	voltage loss due to hydrogen crossover, V
$\eta_{reversible}$	reversible voltage loss, V
$\eta_{irreversible}$	irreversible voltage loss, V

dation. Liu et al. [10] and Aoki et al. [17,18] showed that changing the hydrogen and oxygen partial pressure influenced the fluoride release. This is also echoed in hydrogen peroxide concentration measurements by Chen et al. [19]. High gas partial pressures are also used in typical accelerated chemical degradation tests such as open circuit voltage (OCV) durability testing where a cell is run without drawing load. Gas partial pressures at the membrane/catalyst layer interface are highest when no current is drawn, as shown in several modeling studies [3,20], because the gasses are not depleted by the electricity producing reactions. The higher pressures naturally lead to higher crossover rates and thus accelerate degradation. This type of accelerated experiment has been used by many authors to study the effects of chemical degradation on fuel cell materials [8,16,21–25].

Relative humidity has been also shown to have an impact on membrane permeability and consequently impacts chemical degradation. In general PFSA membranes increase permeability with relative humidity [26–28]. However, studies on the effect of RH show a decrease in degradation with increasing relative humidity [19,29]. Chen et al. [19] postulated that the lower degradation could be a result of lower partial pressures when operating at constant total pressure. Aoki et al. [17,18] showed that changing RH while keeping gas partial pressures constant increased fluoride emission as expected by an increase in gas permeability through the membrane, but also thought there was some contribution from increased H_2O_2 penetration. Finally, Mittal et al. [9], Chen and Fuller [19], and Liu and Zuckerbrod [30] showed that increasing membrane thickness would decrease degradation.

In addition to the parameters of Eq. (1), membrane reactivity to radical groups also plays a significant role in chemical degradation. Studies by Curtin et al. [6] in the case of Nafion® showed that stabilization of the polymer chains was possible by removing reactive end groups which was seen by an improvement in chemical stability when exposed to Fenton's reactions. Finally, temperature increases the reaction rates of the degradation reactions [31] as well as increases membrane permeability.

Though there have been many experimental studies examining fuel cell degradation, there have been fewer attempts to model the different degradation modes. A catalyst layer degradation model has been proposed by Franco and Gerard [32] which modeled voltage stressors and degradation on the cathode catalyst layer. Several finite element models predicting mechanical stresses in the membrane electrode assembly have been proposed by Lee et al. [33], Cleghorn et al. [34], and Huang et al. [35] as well as a catalyst layer delamination model by Kim et al. [36]. Finally, Kundu et al. [24] proposed a semi-mechanistic model for the chemical degradation of GORE-SELECT composite reinforced membranes which modeled fluoride release behaviour using permeability and hydrogen pressure as inputs and also fitted constants related to fluoride ion diffusion and reaction rate constants for membrane degradation. The model was fitted to experimental data and was used to explain fluoride release trends as well as scanning electron microscopy (SEM) observations of the physical damage. A reaction rate model by Shim et al. [37] was also proposed which included both hydrogen and oxygen partial pressure as part of the model.

This study uses open circuit voltage experiments to examine the effect of relative humidity on GORE-SELECT reinforced membranes. Five cells were degraded using open circuit voltage accelerated durability tests, each at a different RH. Initial gas crossover was measured and cumulative fluoride release was monitored. Since many of the tests experienced some interruptions for performance characterization or maintenance, the analysis also includes an understanding of how testing interruptions impact fluoride release data. A semi-empirical model based on previous work by Kundu et al. [24] is used to analyse the experimental results. The ability of the model to simulate fluoride release results of interrupted tests and experiments at different RH is investigated.

2. Experimental

Single-cell fuel cell hardware was supplied by Hydrogenics Corporation each with a geometric active area of 80.1 cm^2. The cells were assembled using Gore™ PRIMEA® series 5510 catalyst coated membranes (CCMs) and proprietary gas diffusion layers (GDL) with microporous layers (MPL). The cells were tested on a Hydrogenics FCATS™ test station, which controlled temperature, humidity, and gas flows. Break-in conditions consisted of holding cell voltage at 0.6 V, with anode and cathode stoichiometries at 2.0 and 2.5 respectively, 100% anode and cathode RH, and a cell temperature of 80 °C.

Table 1
Relative humidity and cell temperature conditions for cells operated at open circuit voltage (OCV).

Cell	Anode/cathode RH (%)	Cell temperature (°C)
1	20	90
2	50	90
3 (Baseline)	75	90
4	75	90
5	100	90

The open circuit voltage (OCV) durability test was conducted at a cell temperature of 90 °C, and no backpressure. Knockout drums were used on the fuel cell outlets to condense and collect water during fuel cell operation. A total of five cells were run under open circuit voltage conditions and are summarized in Table 1. Pure hydrogen was used on the anode and air on the cathode. The anode flow rate was 0.2 standard litres per minute (SLPM—0 °C, 1 atm) and the cathode flow rate was 0.8 SLPM. Cell 3, operated at 75% RH was used as a baseline case for the development of a chemical degradation model and thus will be termed as "Baseline". Cell 4 was a repeat of Cell 3 at 75% RH though it was not allowed to operate as long, 380 versus 860 h. This was to obtain data on how membrane thickness changed with time and provide information on the effect of interruptions.

One issue with any long term durability study are interruptions in testing from the need to perform diagnostic tests (polarization curves), unplanned shutdowns, and test station maintenance. For these reasons it is not always possible to run a cell for hundreds of hours without some shutdowns. Table 2 details the total testing during of the above cells as well as points in testing where a shutdowns or other significant interruption occurred.

The cells were allowed to run for as long as possible to acquire the necessary data, with the exception of Cell 4 which was purposely run to 360 h as a way to examine the progression of degradation. A minimal number of measurements were taken throughout the experiments to reduce the effects of stoppages on the degradation data.

Two types of electrochemical measurement were employed in this study, cyclic voltammetry and hydrogen crossover current. Measurements were performed using an EG&G Princeton Applied Research potentiostat/galvanostat model 273 and Coreware software. For both diagnostic tests humidified hydrogen was passed on the anode, and humidified nitrogen was supplied to the cathode. In cyclic voltammetry measurements the voltage was scanned from 0.1 to 1 V and back to 0.1 V for several cycles with a sweep rate of 20 mV s^{-1}. For measuring hydrogen crossover current, the voltage was scanned from 0.1 to 0.6 V with a sweep rate of 2 mV s^{-1}.

Fluoride ion analysis was carried out using ion chromarography with a Dionex ED40 electrochemical detector working with a Dionex GP40 gradient pump. The minimum detectable fluoride ion concentration was 0.011 ppm.

All effluent water during a fuel cell test was collected using knockout drums between the anode and cathode exits and the test station exhaust. Water was collected daily and stored in polyethylene bottles. Bottles of water were weighed to determine the amount of water deposited during a collection period. Effluent water was then analysed for fluoride ions, in this way the fluoride release rates and cumulative fluoride release from the anode and cathode sides could be determined.

Scanning electron microscopy (SEM) analysis was carried out using a LEO SEM with field emission Gemini Column. The gas diffusion layers were first removed from the membrane electrode assemblies. This was done by repeatedly heating, humidifying and then cooling the MEA until the GDL could be removed easily. Cross-sections were made by freeze fracture from a strip of sample submerged in liquid nitrogen. Once frozen, the sample was broken in half while still submerged. Cross-sections were mounted on the sides of stainless steel nuts so that the fractured side was vertical.

Table 2
Total testing time and points in testing hours where shutdowns or other significant interruption.

Cell	Total testing time (h)	Shutdown/interruption at: (h)
1	478	None
2	756	136
3 (Baseline)	860	436, 519, 734, 744 and 809
4	360	35, 85 and 126
5	918	191

3. Experimental results

3.1. Effect of stoppages

Prior to discussing the effect of RH on degradation it is necessary to discuss the effect of interruptions in testing since many of the experiments in this study, as well as in literature, consist of such interruptions.

Two cells, Cell 3 and Cell 4, were degraded at 75% RH and fluoride release was measured. Unlike the baseline cell (Cell 3), Cell 4 was only operated for 360 was interrupted at 35, 85, and 126 h of operation. The total cumulative fluoride release curves, which combine the contribution from the anode and cathode sides, are shown in Fig. 1 for the baseline experiment (Cell 3) and for Cell 4. The curves show an initial lag followed by an increase in fluoride and finally in the case of Cell 3, a slow-down of the fluoride release is observed. Previous work [24] attributed this lag to the time needed for fluoride ions to be created and diffuse to the channels where they are collected and measured. It is clear from Fig. 1 that even though the two cells were degraded under the same conditions and had similar crossover properties, the fluoride release curves do not match. Cell 3 had a higher total measured cumulative fluoride release than Cell 4. Also, unlike Cell 3 which shows a smooth exponential increase in total cumulative fluoride release over the first 400 h, Cell 4 has an increase in fluoride release followed by nearly a plateau and then another increase.

Typically when cell operation was interrupted, the cell was purged with nitrogen. Further, if a polarization curve was obtained then there was increased water flow through the cell. It is hypothesized that with each interruption the fluoride concentration profiles within the membrane, catalyst layers, and GDL were disrupted and cleared. Thus each time the cell was restarted there was a lag in the fluoride release as concentration profiles were re-established thus underestimating the fluoride release.

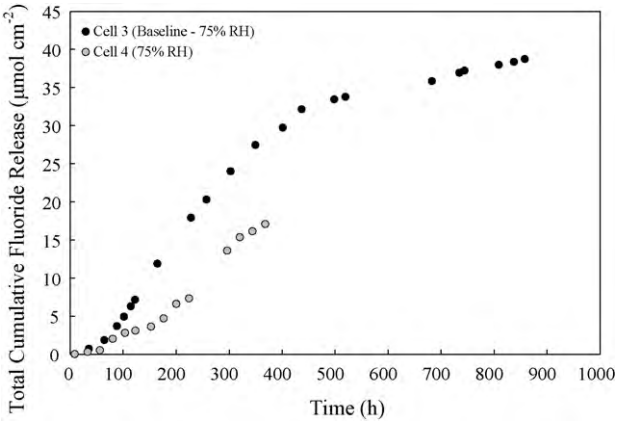

Fig. 1. Comparison of total (anode + cathode) cumulative fluoride release for Cell 3 and Cell 4 (75% RH).

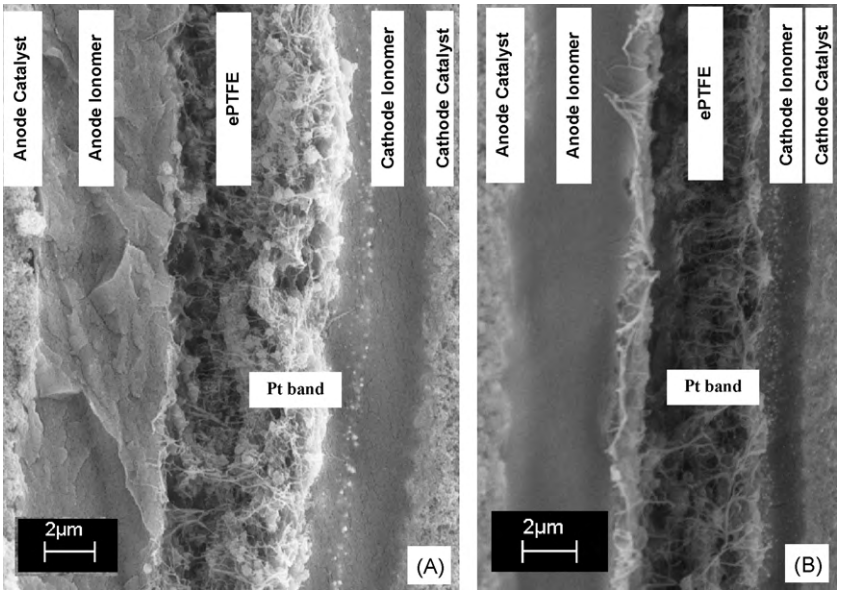

Fig. 2. Comparison of SEM cross-sections of two degraded Gore CCMs from (A) Cell 4 after 360 h, 75% RH, and (B) Cell 3, baseline cell after 860 h, 75% RH.

SEM images of the catalyst coated membranes of Cell 4 and Cell 3 are shown in Fig. 2. Overall, Cell 4, which operated for 360 h, showed significantly less degradation than Cell 3 which was operated for 860 h. Analysis of SEM results showed that both cells had cathode side thinning. Furthermore, in Cell 4 there was no anode thinning. This reinforces the assertion of previous work [24] that the observed degradation and fluoride ion release originates in the cathode electrolyte layer.

3.2. Effect of RH

The effect of RH on total cumulative fluoride release was measured by testing Cells 1, 2, 3 and 5 at 20%, 50%, 75%, and 100% RH respectively. Previous work [24], has shown that the hydrogen crossover rate is an important factor for chemical degradation. The hydrogen crossover rate was measured electrochemically as described and the resultant crossover currents for each cell are shown in Table 3.

It has been shown that hydrogen permeability increases with increasing relative humidity in GORE^{TM} reinforced membranes [28] and it is also known that under constant total pressure conditions the partial pressure of a gas will decrease with increasing relative humidity. The result is an overall decrease in hydrogen crossover with increasing relative humidity. This was confirmed in one cell test (Cell 5) where the H_2 crossover currents were measured at varying relative humidity (see Fig. 3).

The crossover measurements for each cell, tested at the experimental RH, generally follow this trend though Cell 5 (100% RH) deviates slightly by having a higher crossover rate than Cell 3 (75% RH). This behavior is attributed to cell-to-cell variability where such variability is more influential to initial gas crossover than humidity conditions alone. Cells 1–3 have consistent hydrogen crossover rates with Fig. 3.

The total (anode + cathode) cumulative fluoride release for the four CCMs used in this study is shown in Fig. 4. Though not shown,

Table 3
Hydrogen crossover rates of Cells 1–3, and 5 at their respective test relative humidity.

Cell	Anode/cathode RH%	Crossover current, mA cm^{-2}
1	20	2.40
2	50	2.36
3 (Baseline)	75	1.98
5	100	2.08

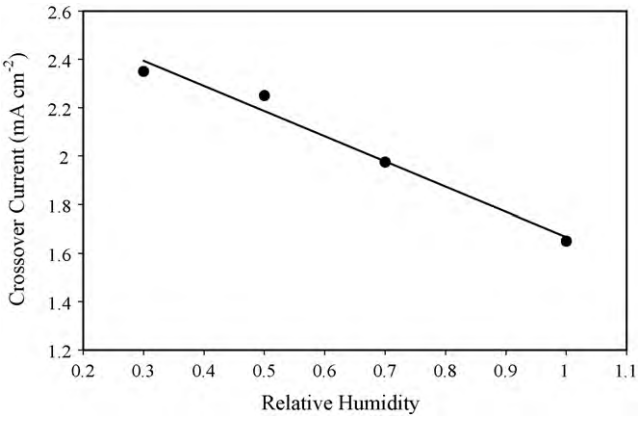

Fig. 3. Effect of changing RH on hydrogen crossover current at constant total pressure.

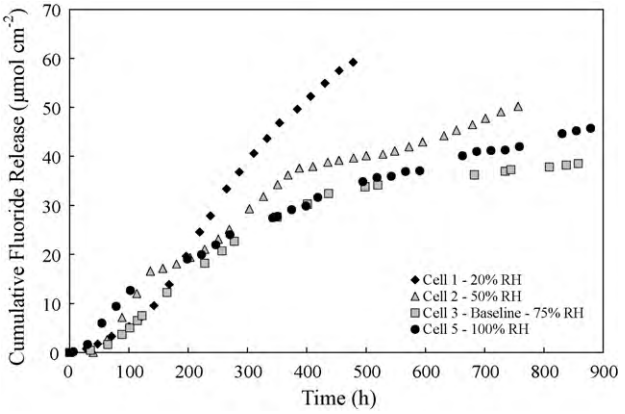

Fig. 4. Total (anode + cathode) cumulative fluoride release for Cell 1 (20% RH), Cell 2 (50% RH), Cell 3 (75% RH), and Cell 5 (100% RH).

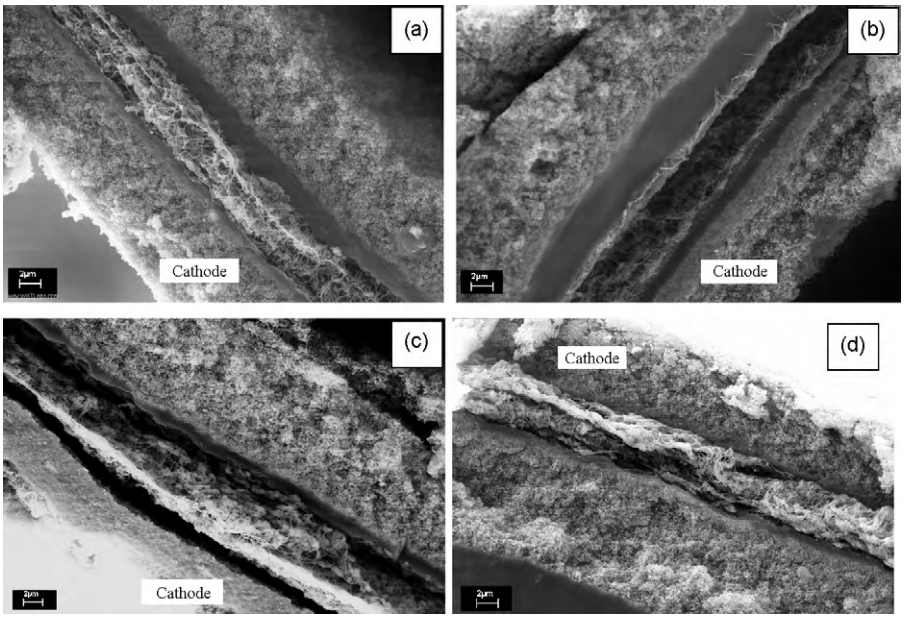

Fig. 5. SEM images of degraded membranes from (a) Cell 5 (100% RH), (b) Cell 3 (75% RH), (c) Cell 2 (50% RH), and (d) Cell 1 (20% RH).

anode fluoride release was lower than cathode release indicating that cathode side degradation was predominant in all cells.

Overall, the total cumulative fluoride release showed some lag time which is attributed to the time necessary for fluoride ions to be produced within the fuel cell and then diffuse to the channels. It has been postulated the cumulative release rates begin to slow when the cathode electrolyte has been completely consumed [24], and the degradation front has moved into the reinforcement layer towards the anode electrolyte layer.

The total (anode + cathode) cumulative fluoride release effectively represents the amount the electrolyte membrane has degraded. From Fig. 4 it can be seen that after long testing durations the order of Cells from highest total cumulative fluoride release to lowest is Cell 1(20% RH), Cell 2 (50% RH), Cell 5 (100% RH), and Cell 3 (75% RH). Though as discussed, interruptions will have some impact. The degree of the impact will be discussed in the following section with the use of a semi-empirical model. It is not expected to influence the overall trends significantly since Cells 2 and 4 only experienced one interruption and all of the interruptions in Cell 3 were late in life.

The relationship between the total cumulative fluoride release and membrane morphology can be seen with scanning electron microscopy. Characteristic SEM images are shown in Fig. 5. The membranes used in this study contain a reinforcement layer which bisects the membrane. The electrolyte closest to the anode catalyst layer is referred to as the anode electrolyte, and similarly the cathode electrolyte refers to the electrolyte closest to the cathode catalyst layer. The results show that after testing, Cell 3 (75% RH) had significant cathode electrolyte degradation and minimal anode electrolyte degradation.

Cell 5 (100% RH) had significant cathode electrolyte degradation and some anode electrolyte degradation. Finally, Cells 1 (20% RH) and 2 (50% RH) both had extensive degradation of the anode and cathode electrolytes. Some anode electrolyte could still be observed in Cell 2; however, there was no observable cathode or anode electrolyte in Cell 1.

The OCV versus time curves for each of the four membranes are shown in Fig. 6. The curves show degradation consistent with the fluoride release data. Initially, voltage values begin above 0.9 V and rapidly decrease. This initial transient period has been shown to be primarily the result of reversible voltage losses and in a smaller part it is attributed to irreversible voltage losses promoted by the permanent degradation of the catalyst layer and ionomer [24]. After approximately 150 h the voltage degradation rate begins to stabilize and enters a steady degradation period which can be considered irreversible voltage losses caused by material degradation.

The mechanism of degradation for these membranes has been proposed previously [24]. It is briefly described here with reference to Fig. 7. Hydrogen crossover from the anode to the cathode is considered to be primarily responsible for the observed degradation. It is proposed that at the cathode electrolyte/catalyst layer interface the crossed-over hydrogen promotes the production of hydroxyl radicals. The radicals are then able to penetrate into the electrolyte layer and cause its degradation thus producing fluoride ions, and creating a "degradation front". With degradation, the electrolyte layer begins to thin causing the observed cathode electrolyte thinning. The electrolyte layer can thin to a point where radicals may penetrate into the reinforcement layer. It is also postulated that because of the inert nature of the reinforcement and the small amount of electrolyte in the pore spaces the fluoride release rate slows because of lack of reactants. After long times, the degradation

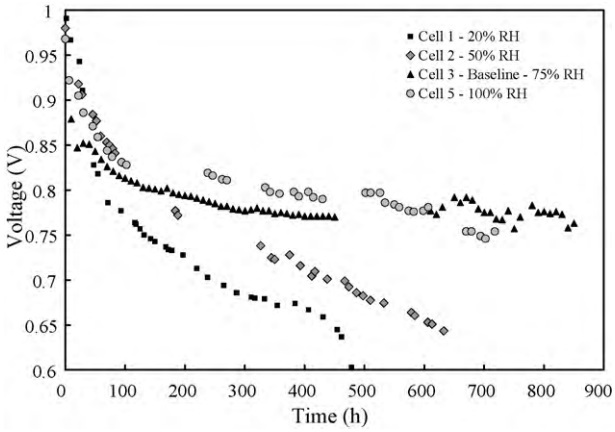

Fig. 6. Open circuit voltage lifetime testing for Cell 1 (20% RH), Cell 2 (50% RH), Cell 3 (75% RH), and Cell 5 (100% RH).

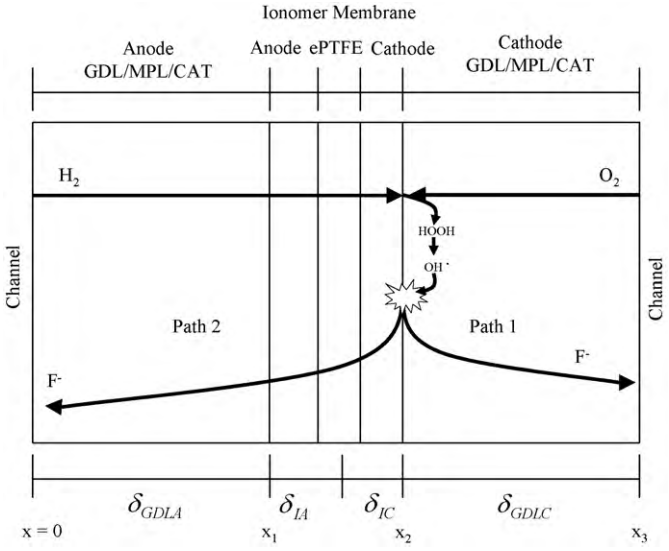

Fig. 7. Model domain and processes highlighting fluoride ion transport pathways.

front will move through the anode electrolyte as seen in Fig. 5c and d and the fluoride release rate may increase.

4. Degradation mechanism and model

The fluoride release behaviour was modeled using a semi-mechanistic chemical degradation model similar to that in [24]. It is assumed that hydrogen and oxygen react near the cathode catalyst layer to produce radical species which then degrade the membrane. Fluoride ions generated by the degradation process are transported out of the fuel cell by two paths. In one case, Path 1, fluoride diffuses from the generation point through the cathode catalyst layer, cathode MPL and GDL to the channels. Path 2, consists of the fluoride ions diffusing through the ionomer membrane towards the anode, then through the remaining anode layers to the anode channels. In order to simplify the system four main areas will be considered as shown in Fig. 7. The anode and cathode GDL/MPL/catalyst layers will be two such blocks, and the electrolyte membrane will be split into an anode block and a cathode block.

The rate of hydrogen crossover is determined by the permeability of the membrane, the partial pressure difference across the membrane and the thickness of the electrolyte membrane layers. This hydrogen flux, N_{H_2}, can be calculated by Eq. (2) and it is related to the crossover current measured during linear sweep voltammetry tests by (3).

$$N_{H_2} = P_{M,H_2}\frac{\Delta p_{H_2}}{\delta_m} \tag{2}$$

$$i_{H_2} = P_{M,H_2}(2F)\frac{\Delta p_{H_2}}{\delta_m} = P'_{M,H_2}\frac{\Delta p_{H_2}}{\delta_m} \tag{3}$$

Once at the reaction site, hydrogen and oxygen react to form peroxide and radicals. The rate at which radicals are produced, N_{OH}, is proportional to the permeation rates of hydrogen and oxygen and is described by Eq. (4).

$$\begin{matrix} N_{OH}\,\alpha\,N_{H_2} \\ \text{and} \\ N_{OH}\,\alpha\,N_{O_2} \end{matrix} \tag{4}$$

Radicals degrade the polymer electrolyte membrane and produce fluoride ions as a product. The rate of degradation of the electrolyte is related to the rate of OH radical production as well as the amount of electrolyte available for reaction. This model focuses only on the rate of degradation of the cathode electrolyte since the ePTFE layer likely presents a barrier to OH radical diffusion to the anode electrolyte layer. The rate of electrolyte consumption is therefore considered to be related to the rate of radical production and the amount of cathode electrolyte. The amount cathode electrolyte is represented as a fraction, f_I, of the mass of cathode electrolyte at $t = 0$ h, as shown in Eq. (5).

$$-\frac{df_I}{dt}\alpha(N_{OH})(f_I) \tag{5}$$

Substituting the hydrogen and oxygen fluxes and a proportionality constant yields Eq. (6):

$$-\frac{df_I}{dt} = K_0(N_{H_2})(N_{O_2})(f_I) \tag{6}$$

where K_0 is a proportionality constant relating the hydrogen flux and electrolyte fraction to the electrolyte degradation rate. This degradation rate determines the rate of fluoride production as well as the rate of thickness change of the cathode ionomer.

Oxygen and hydrogen permeation rates are related to each other through the membrane selectivity. Thus Eq. (6) can be re-written as:

$$-\frac{df_I}{dt} = K_1(N_{H_2})^2(f_I) \tag{7}$$

where K_1 is a proportionality constant. The rate of fluoride ion generation is related to the rate of electrolyte degradation through the polymer chain structure. For every milligram of ionomer that is degraded per second, a certain amount of fluoride will be generated at the point of degradation depending on the exact chemical make-up of the polymer chain. Eq. (8) relates the amount of fluoride produced to the fractional loss of electrolyte by a proportionality constant. Physically this constant would be related to the number of fluorine atoms in the electrolyte chain structure.

$$\frac{dn_{F^-}}{dt} = -K_2\frac{df_I}{dt} \tag{8}$$

Fluoride ions, once generated, are considered to be transported to the bipolar plates by two paths, Path 1 and Path 2, as previously described. The rate at which these processes occur depends on the concentration gradients in the different layers. These gradients are time-dependant and are modeled as by Fick's law as shown in Eq. (9).

$$\frac{dC_{F^-}}{dt} = D_i\frac{d^2C_{F^-}}{dx^2} \quad \text{where, } D_i = \begin{cases} D_{GDL}, 0 < x < x_1 \\ D_I, x_1 < x < x_2 \\ D_{GDL}, x_2 < x < x_3 \end{cases} \tag{9}$$

At the generation site, x_2, it is assumed that there is no accumulation of fluoride and as such the fluoride generation rate is balanced by the flux of fluoride diffusing away from the site by the two transport paths (1 and 2) as shown in Eq. (10).

$$N_{F^-}\big|_{x_2} = [N_{F^-}]_{Path\,1} + [N_{F^-}]_{Path\,2} \tag{10}$$

Further, the flux of fluoride out of the GDL and into the channel is described by Eq. (11). It is assumed that at the channels the fluoride is quickly washed away and therefore the concentration is effectively zero.

$$N_{F^-} = D_{GDL}\frac{dC_{F^-}}{dx} \tag{11}$$

Finally, the cumulative fluoride release into the cathode or anode channels is given by (12).

$$F_C = \int_0^t N_{F^-}\,dt \tag{12}$$

Degradation of electrolyte material is only considered to result in a change of cathode electrolyte membrane thickness. As such cathode electrolyte thickness, as a fraction of the initial thickness,

Table 4
Model parameters for the degradation model.

Variable	Value
Δp_{H_2}	364.4 mm Hg
δ_{IA}	7.5×10^{-4} cm
δ^0_{IC}	7.5×10^{-4} cm
P'_{M,H_2}	1.9×10^{-8} A cm cm^{-2} mm Hg^{-1}
K_1	2.9×10^{-2} mol^{-2}
K_2	4.7×10^{-7} mol cm^{-2}
D_{GDL}	4.2×10^{-9} cm^2 s^{-1}
D_I	1.2×10^{-10} cm^2 s^{-1}
δ_{GDL}	4×10^{-3} cm

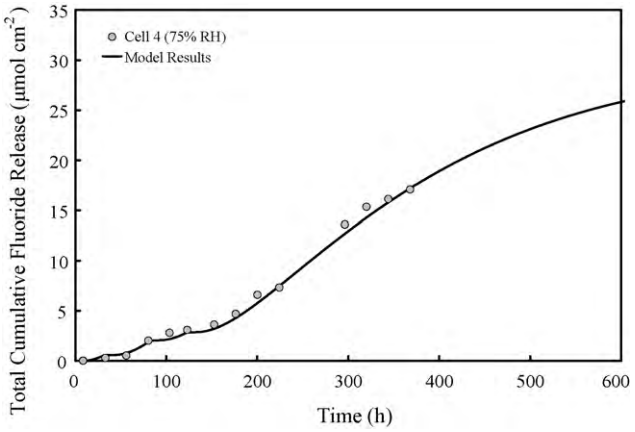

Fig. 8. Total (anode + cathode) cumulative fluoride release results for Cell 4. Solid lines represent model predictions.

is related to the fraction of cathode electrolyte mass. The total electrolyte membrane thickness is therefore the anode thickness and remaining cathode thickness as shown in (13). As the thickness changes with time, permeability can be calculated by Eq. (3).

$$\delta_m = \delta_{IA} + \delta^o_{IC} f_I \tag{13}$$

To simulate the effect of stoppages and purging, the model was first allowed to run until a stoppage time. For Cell 4 at 35, 85, and 126 h all fluoride concentrations were reset to 0 and the simulation was restarted. Variables such as the fraction of cathode electrolyte remaining were not reset.

5. Model results

The above model was fitted to the results for Cell 3 (75% RH). The parameters and resultant fit parameters used are given in Table 4.

Once fitted, the model was used to simulate fluoride release results for Cells 1, 2, 4 and 5. When simulating the results of other cells the only input parameters that were changed were the permeability which was measured for each membrane, and hydrogen partial pressure which was specific for each test RH condition.

5.1. Effect of interruptions

Total cumulative fluoride release (anode + cathode) experimental results and simulation predictions are shown in Fig. 8 for Cell 4. Recall that conditions for cell Cell 3 and four were similar though the fluoride release trends were not. This was attributed to inter-

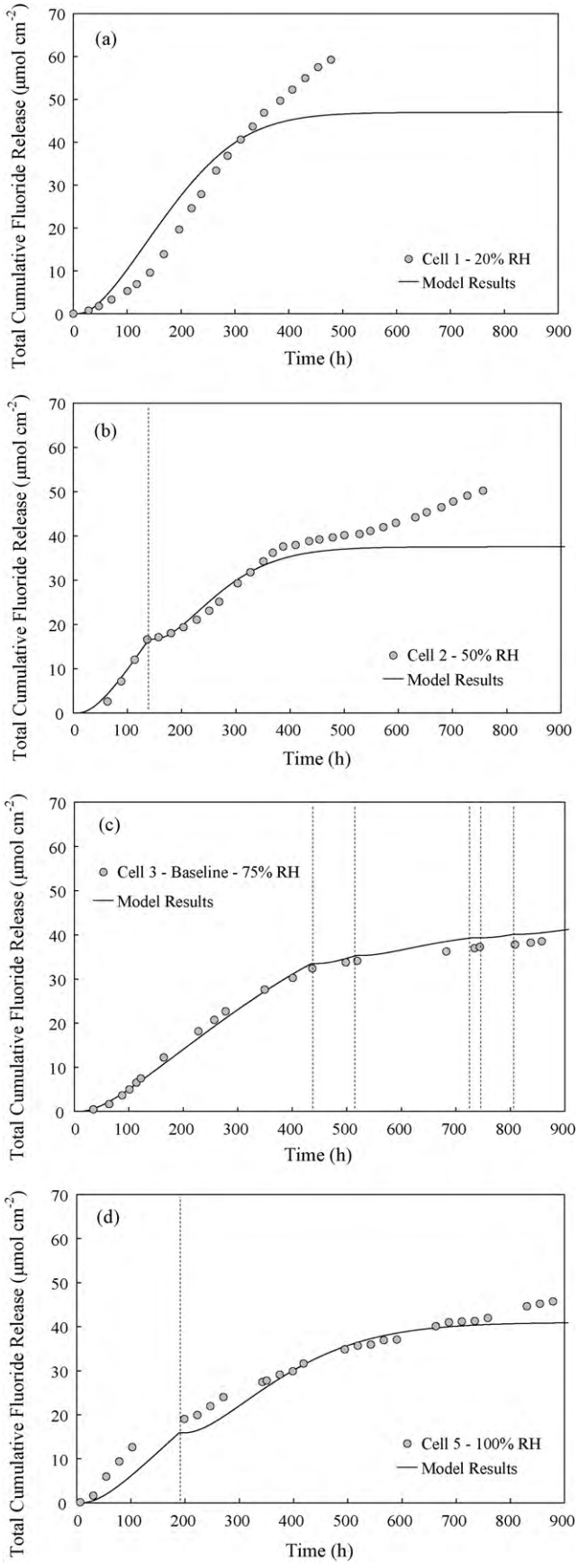

Fig. 9. Total (anode + cathode) cumulative fluoride release experimental and model results using the second order model for (a) Cell 1, (b) Cell 2, (c) Cell 3, and (d) Cell 5. The model was fit to data from Cell 3 and then applied to Cells 1, 2 and 5 without further fitting. Testing interruptions were accounted for in each case. Dotted vertical lines indicate when cell interuptions took place.

ruptions in testing causing fluoride concentration profiles to be disrupted resulting in a lag time for fluoride measurement when tests were restarted. Results for Cell 3 are shown in Fig. 9c. The model was able to effectively simulate the total release data for Cell 4. This confirms that the discrepancy between the fluoride release behaviour of Cell 3 and Cell 4 is due to the stoppages which changed the fluoride release trends.

A broader implication of the above result is that any stoppage in tests involving membrane degradation may influence the observed fluoride release results. This factor is typically not controlled for in other degradation studies in the literature and it is unknown what the impact would be.

5.2. Effect of RH

The model, along with consideration of the effect of testing interruptions, was also applied to the fluoride release results for cells operated at different RH. The model simulations, fitted to the results of Cell 3, show good agreement with experimental data for Cells 1, 2, and 5 with the exceptions described below. Model simulation results for Cell 1 are higher than experimental data at early degradation times. This is due to changes in membrane and GDL fluoride diffusivities where at the very low RH fluoride ion diffusion is impeded by the lack of water and a longer lag time is observed. However, the slope of the two cumulative fluoride release curves are similar at early times. In all the simulations, the model underpredicts fluoride release after long degradation times. It is believed that at longer times anode electrolyte degradation starts to contribute significantly to the fluoride release which is not accounted for in the model. Recall from the SEM images (Fig. 5) the extent of anode electrolyte degradation in Cell 2 and especially in Cell 1 and to a lesser extent Cells 3 and 5. From a practical standpoint this is not a significant limitation in the model since in most fuel cell applications, the system would have been considered to have failed long before such extensive degradation, based on performance or crossover failure criteria. The model is also able to capture the higher fluoride release of Cell 5 over Cell 3 due to the higher initial hydrogen crossover rate of Cell 5 (see Table 1).

The above results show that the initial crossover rate is an important factor which influences degradation at moderate to high relative humidity. The effect of relative humidity on permeability and hydrogen partial pressure are also important since they contribute to the overall crossover rate. A higher initial hydrogen crossover accelerates the degradation cycle of thinning and crossover resulting in the above results. This is consistent with a study by Pierpoint and coworkers who correlated initial fluoride release rate to cell lifetime [38]. Since there is a relationship between the initial crossover rate and initial fluoride release rate as described in the model formulation, the initial crossover rate should also be a strong indicator of durability in cases where no current is drawn. This held true for the cells tested in the above work.

6. Conclusions

In this study the effect of RH on chemical degradation of the ionomer membrane was studied. Gore™ PRIMEA® series 5510 catalyst coated membranes were degraded using an open circuit voltage durability experiment at 90 °C, and 20%, 50%, 75%, and 100% anode/cathode relative humidity.

Two cells, Cells 3 and 4, were degraded at 75% RH but for different total times, 860 and 360 h respectively. SEM analysis of showed that degradation was located near the cathode catalyst layer and that degradation over 360 h showed less ionomer thinning. Cumulative fluoride release results showed different trends between the samples which was attributed to interruptions in testing resulting in a disruption of fluoride concentration profiles within the MEA. MEAs degraded at different RH showed that with lower relative humidity the fluoride release rate and damage to the ionomer, as seen in SEM images, increased which was attributed to an overall increase of hydrogen crossover at lower RH.

A semi-mechanistic model was used to model the fluoride release results. Interruptions in testing were modeled by resetting fluoride concentrations throughout the modeled domain. The model was fitted to the fluoride release results of Cell 3, the baseline case at 75% RH and then used to simulate results at other RH. The model was able to predict the fluoride release results of Cell 4 when the effect of interruptions were included in the model. The model predictions also showed reasonable agreement with fluoride release curves at different RH, for Cells 1, 2, and 5, when inputted with beginning of life crossover information and RH.

Acknowledgements

The authors would like to acknowledge the Natural Sciences and Engineering Research Council (NSERC) of Canada for financial support.

References

[1] M.F. Mathias, R. Makharia, H.A. Gasteiger, J.J. Conley, T.J. Fuller, C.J. Gittleman, S.S. Kocha, D.P. Miller, C.K. Mittelsteadt, T. Xie, S.G. Yan, P.T. Yu, Electrochem. Soc. Interf. 14 (2005) 24–36.
[2] T. Kinumoto, M. Inaba, Y. Nakayama, K. Ogata, R. Umebayashi, A. Tasaka, Y. Iriyama, T. Abe, Z. Ogumi, J. Power Sources 158 (2006) 1222–1228.
[3] P. Rama, R. Chen, R. Thring, Proc. Inst. Mech. Eng. Part A (J. Power Energy) 220 (2006) 535–550.
[4] R. Borup, J. Meyers, B. Pivovar, et al., Chem. Rev. 107 (2007) 3904–3951.
[5] F.A. de Bruijn, V.A.T. Dam, G.J.M. Janssen, Fuel Cells 8 (2008) 3–22.
[6] D.E. Curtin, R.D. Lousenberg, T.J. Henry, P.C. Tangeman, M.E. Tisack, J. Power Sources 131 (2004) 41–48.
[7] N.E. Cipollini, ECS Trans. 11 (2007) 1071–1082.
[8] A. Ohma, S. Suga, S. Yamamoto, K. Shinohara, J. Electrochem. Soc. 154 (2007) 757–760.
[9] V.O. Mittal, H.R. Kunz, J.M. Fenton, J. Electrochem. Soc. 153 (2006) 1755–1759.
[10] H. Liu, J. Zhang, F.D. Coms, W. Gu, B. Litteer, H.A. Gasteiger, ECS Trans. 3 (2006) 493–505.
[11] A. Ohma, S. Suga, S. Yamamoto, K. Shinohara, ECS Trans. 3 (2006) 519–529.
[12] W. Bi, G.E. Gray, T.F. Fuller, Electrochem. Solid-State Lett. 10 (2007) B101–B104.
[13] N. Hasegawa, T. Asano, T. Haranaka, M. Kawasumi, Y. Morimoto, ECS Trans. 16 (2008) 1713–1716.
[14] T. Sakai, H. Takenaka, N. Wakabayashi, Y. Kawami, E. Torikai, J. Electrochem. Soc. 132 (1985) 1328–1332.
[15] H.B. Park, S.Y. Nam, J.W. Rhim, J.M. Lee, S.E. Kim, J.R. Kim, Y.M. Lee, J. Appl. Polym. Sci. 86 (2002) 2611–2617.
[16] S. Kundu, M. Fowler, L.C. Simon, J. Power Sources 180 (2008) 760–766.
[17] M. Aoki, H. Uchida, M. Watanabe, Electrochem. Commun. 8 (2006) 1509–1513.
[18] J.J.A. Kadjo, J.P. Garnier, J.P. Maye, F. Relot, S. Martemianov, Russ. J. Electrochem. 42 (2006) 467–475.
[19] C. Chen, T.F. Fuller, ECS Trans. 11 (2007) 1127–1137.
[20] M. Seddiq, H. Khaleghi, M. Mirzaei, J. Power Sources 161 (2006) 371–379.
[21] S. Hommura, K. Kawahara, T. Shimohira, 207th Meeting of the Electrochemical Society—Meeting Abstracts, 2005, p. 803.
[22] T.A. Aarhaug, A.M. Svensson, ECS Trans. 3 (2006) 775–780.
[23] A. Ohma, S. Yamamoto, K. Sinohara, ECS Trans. 11 (2007) 1181–1192.
[24] S. Kundu, M. Fowler, L.C. Simon, R. Abouatallah, N. Beydokhti, J. Power Sources 183 (2008) 619–628.
[25] S. Kundu, M. Fowler, L.C. Simon, R. Abouatallah, J. Power Sources 182 (2008) 254–258.
[26] P. Gode, G. Lindbergh, G. Sundholm, J. Electroanal. Chem. 518 (2002) 115–122.
[27] K. Broka, P. Ekdunge, J. Appl. Electrochem. 27 (1997) 117–123.
[28] S. Cleghorn, J. Kolde, W. Liu, in: W. Vielstich, H. Gasteiger, A. Lamm (Eds.), Handbook of Fuel Cells—Fundamentals, Technology and Applications, vol.3, John Wiley & Sons, New York, 2003, pp. 566–575.
[29] C.H. Paik, T. Skiba, V. Mittal, S. Motupally, T.D. Jarvi, 207th Meeting of the Electrochemical Society—Meeting Abstracts, 2005, p. 771.
[30] L. Wen, D. Zuckerbrod, J. Electrochem. Soc. 152 (2005) 1165–1170.
[31] A.B. LaConti, M. Hamdan, R.C. McDonald, in: W. Vielstich, H. Gasteiger, A. Lamm (Eds.), Handbook of Fuel Cells—Fundamentals, Technology and Applications, vol.3, John Wiley & Sons, New York, 2003, pp. 647–663.

[32] A.A. Franco, M. Gerard, J. Electrochem. Soc. 155 (2008) B367–B384.
[33] S.J. Lee, C.D. Hsu, C.H. Huang, J. Power Sources 145 (2005) 353–361.
[34] Y. Tang, M.H. Santare, A.M. Karlsson, S. Cleghorn, W.B. Johnson, J. Fuel Cell Sci. Tech. 3 (2006) 119–124.
[35] X. Huang, R. Solasi, Y. Zou, M. Feshler, K. Reifsnider, D. Condit, S. Burlatsky, T. Madden, J. Poly. Sci. Poly. Phys. 44 (2006) 2346–2357.
[36] S. Kim, M. Khandelwal, C. Chacko, M.M. Mench, ECS Trans. 16 (2008) 1977–1986.
[37] J.Y. Shim, S. Tsushima, S. Hirai, ECS Trans. 16 (2008) 1705–1712.
[38] D. Pierpont, M. Hicks, T. Watschke, P. Turner, ECS Trans. 1 (2005) 229–237.